Nondestructive Evaluation of Ceramics Systems

DAMAGE SENSITIVITY AND ACOUSTIC EMISSION OF SIC/SIC COMPOSITE DURING TENSILE TEST AND STATIC FATIGUE AT INTERMEDIATE TEMPERATURE AFTER IMPACT DAMAGE

Matthieu Picard, Emmanuel Maillet, Pascal Reynaud, Nathalie Godin, Mohamed R'Mili, Gilbert Fantozzi, Jacques Lamon
INSA-Lyon, MATEIS CNRS UMR 5510, 7 Avenue Jean Capelle, F-69 621 Villeurbanne, France.

ABSTRACT

This paper discusses the tensile resistance of an impact-damaged SiC/SiC based ceramic composite. As-received and impact-damaged specimens were subjected to static fatigue tests at 650°C and 450°C and to monotonous tensile tests at room temperature. Damage induced during the tensile and fatigue tests was characterized by the evolution of linear density of acoustic emission events (AE) during unloading-reloading cycles. Results of tensile tests at room temperature show the material impact insensitivity and the analysis of AE signals has demonstrated efficiency for proper investigation of damage evolution in the impacted specimens. During fatigue at 450°C, 650°C and under 80 MPa, both impact-damaged and as-fabricated samples survived 1000 hours. Residual strengths indicated insensitivity to impact damage. At 650°C, damage evolution seemed to slow down from matrix self-healing.

INTRODUCTION

Due to low weight/mechanical properties ratios and high temperature strength, ceramic matrix composites (CMCs) are very attractive candidates for civil aircrafts applications. For these applications, resistance to foreign object damage (FOD) is a key issue to insure structural reliability in service. In the literature, a few authors have investigated the FOD response of 2D woven CMC[1-5]. They have shown that low energy impact was equivalent to quasi-static indentation and that a conical damage zone was created.

Meanwhile, investigations by Ogi *et al.*[6] and Herb *et al.*[7] on 3D woven CMC have shown that tri-dimensional fibre architectures prevent the material from delamination so that the damaged cone remains limited and well delineated. After indentation (*i.e.* ballistic[1-6] or quasi-static impact tests[7]), residual strengths were measured using tensile or flexural tests at room temperature[1-4,6,7].

Few works on the effect of impact damage on composite lifetime under fatigue at elevated temperature have been reported. Recently, Verrilli *et al.*[5] have performed cyclic fatigue tests on 2D cross ply SiC/SiC composite at 1316°C after impact tests at 1200°C. They have observed that lifetime decreases tremendously with increasing impact energy. After high energy impact damage the average lifetime was 40 times smaller than that obtained after low energy impact tests. However, impact damage evolution during fatigue has not been studied in real time.

This paper investigates the evolution of impact damage during fatigue at high temperature on a 3D SiC/SiC composite using acoustic emission signals and the sensitivity to impact damage. Acoustic emission data were analyzed using homemade software that determines the spatial distribution of AE events during the tests. As-fabricated and impact-damaged specimens were tested at room and at high temperatures (*i.e.* 450°C and 650°C).

EXPERIMENTAL PROCEDURE

Material and specimen preparation

The SiC/SiC composite investigated (manufactured by Snecma Propulsion Solide - SAFRAN Group (Bordeaux, France)) was made of an interlock preform of plies of 0/90 yarns woven in a 8 HSW pattern[8] with a self-healing [Si-B-C] matrix. The fibres were coated by a PyC layer deposited via chemical vapour infiltration[8]. This 3D fibrous preform (Guipex® preform) improves the through thickness properties[9]. Yarns contain 500 SiC Nicalon fibres. The fibre volume fraction was between 35% and 40% and the porosity volume fraction was around 12%. A barrier coating protected sample surface against oxidation.

Rectangular test specimens were machined out of 1.8 mm thick panels: specimens' dimensions were 24 mm in width and 200 mm in length. Impact damage was generated by quasi-static indentation by Herb *et al.*[7]. A hemispherical steel punch with a 9 mm diameter was used. The specimens were clamped as shown on Figure 1.

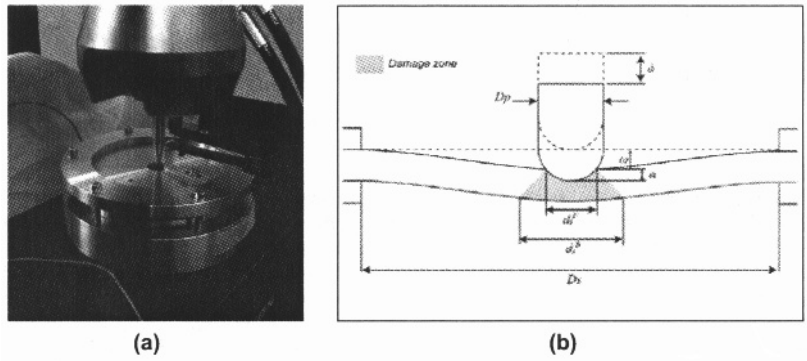

Figure 1. (a) Quasi-static indentation indentation with D_s=18 and D_p= 9 mm. (b) Schematic view of specimen loading (from Herb *et al.*[7]).

Figure 2 shows the cone crater that had been created. Breakage of fibre bundles was observed on back side (Figure 2a), and the impact side (Figure 2b). On the impact side, the sample displayed a neat circular mark. Images of the impact and back sides were post-treated using the Image J software, in order to measure cone area on each side of samples. It was found to be about 33 mm^2 on the front side which is equivalent to a hole with a diameter of 6.5 mm. On the back side, the damaged area was about 85 mm^2 which is equivalent to a hole with a 10.5 mm diameter. The cone crater was sharply delineated, which can be attributed to the 3D fibrous architecture of material and the resulting absence of delamination.

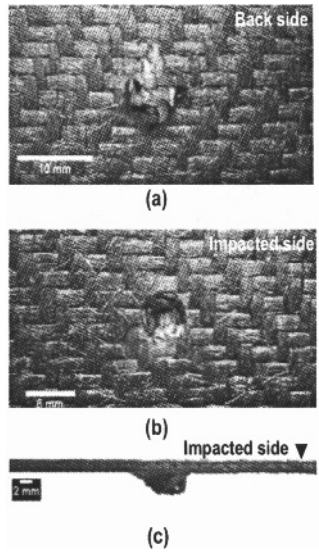

Figure 2. Optical photographs of the SiC/SiC specimens after quasi static indentation: (a) back side (d_i^B= 10.5 mm) (b) impacted side (d_i^F = 6.5 mm) (c) thickness view.

Post-indentation mechanical testing

Static fatigue and tensile experiments were performed using a 25kN uniaxial pneumatic tensile loading machine with one direction of fibres parallel to the loading direction. Specimen elongation was measured using an extensometer (gauge length = 32 mm).

Static fatigue tests were carried out at 450°C and 650°C under air, with uniform temperature in the gauge length (cold grips). Specimens were heated up to the test temperature at a rate of 20°C/min. The load was applied after 2 hours, when the gauge length was expected to be at the test temperature. During the static fatigue tests, specimens were first loaded at a constant rate of 1200 N/min up to the test load corresponding to 80 MPa, close to the elastic limit of composite.

Tensile tests under monotonous loading were performed at room temperature, on impacted specimens (post-impact strength) and on specimens after 1000 hours of static fatigue (residual strength). For all the tests, damage was characterized using periodical unloading-loading cycles (every 12 hours during the static fatigue tests) and also acoustic emission signals. For comparison purposes, a few tests were performed on as-fabricated specimens.

Acoustic emission monitoring

AE was monitored using a MISTRAS 2001 data acquisition system (Euro Physical Acoustics). Two MICRO-80 sensors were positioned directly on the specimen, inside the grips, using vacuum grease with a medium viscosity as a coupling agent. Acquisition parameters were set as follows: pre-amplification 40 dB, threshold 36 dB, peak definition time 50 µs, hit definition time 100 µs, hit lockout time 1000 µs[10,11]. AE signal parameters (amplitude, energy, duration, counts, location…) as well as time, load and strain were measured in real time by the data acquisition system.

As depicted by Figure 3, the zone of interest for the AE events was 80 mm long and located on each side of the mid-plane. Since two sensors only were used, the longitudinal positions of AE origins were determined (see Figure 3a).

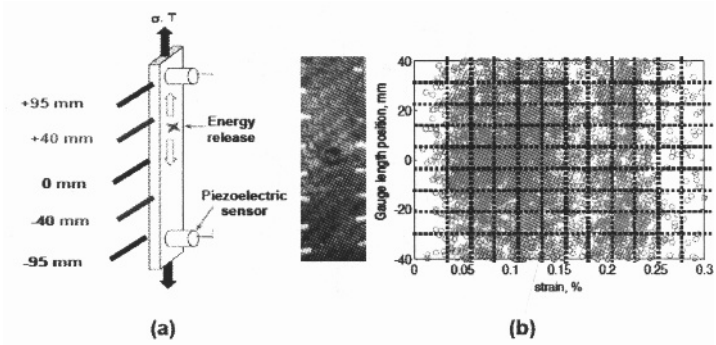

Figure 3. (a) Specimen and Acoustic Emission setting (b) Locations of AE sources in a tensile specimen versus strain. Also shown is the grid defined in order to determine the linear density of counts of acoustic events along specimen axis during tensile tests or static fatigue tests.

AE sources locations were derived using AE wave velocity, that was measured using a pencil lead break procedure: 9100 m/s for both the as-fabricated and the impact-damaged specimens. Morscher *et al.*[12] showed that in ceramic matrix composites wave velocity decreases with increasing stress-induced damage. Wave velocity value was corrected using the attenuation coefficient

$$\gamma = (E/E_0)^{0.5} \qquad (1)$$

E is the secant elastic modulus determined from unloading-reloading hysteresis loops and E_0 is the initial elastic modulus.
AE data were post-treated using dedicated software, which provides linear density along specimen axis of acoustic events during the tests[13]. This analysis of acoustic emission is non-trivial. It is useful to identify the most active zones during the tests.

RESULTS AND DISCUSSION

Effect of impact-damage on tensile behaviour

During the tensile tests, the impacted specimens failed from the mid-plane whereas the as-fabricated samples failed from the upper or lower parts of the gauge length. Figure 4a shows typical tensile curves. For both the as-fabricated and the impact-damaged specimens, the stresses were determined from the net-section of samples:

$$\sigma = F/\, b\,(w-a) \qquad (2)$$

where F is the force on specimen, w is specimen width, a is the average diameter of crater, $b = 1.1$ mm is specimen effective thickness (sealcoat was not taken into account since it did not contribute to the mechanical resistance). As shown by Figure 4a, for all the samples, the tensile response was non-linear, beyond the proportional limit, as a result of stress-induced matrix cracking. The two impacted specimens exhibited higher stresses (or smaller deformations) and a slightly smaller ultimate strength compared to as-fabricated specimens (Figure 4a): ultimate strength was 80% of the reference, whereas strain-to-failure was reduced by 50% (Table 1).

Table 1. Failure stresses and strains measured on the impact-damaged and as-fabricated specimens at room temperature.

Sample	Failure strain (%)	Failure stress * (MPa)
Not-impacted	0.64	275
Impacted-1	0.30	245
Impacted-2	0.28	231

To evaluate the impact damage sensitivity strength data were plotted with respect to average cone diameter size according the classical equation for notch sensitivity, which indicates that the stress at failure at hole tip is equal to the strength of specimen without hole:

$$\sigma_R(a) = \sigma_R(a = 0)\,(1-a/w) \qquad (3)$$

where a is average diameter of cone (figure 1b), σ_R is the failure stress given by F/wb.

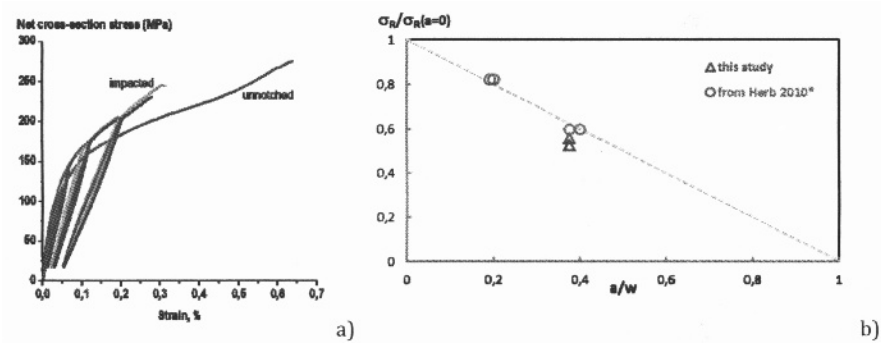

Figure 4. (a) Tensile behaviour of impact-damaged and as-fabricated specimens. (b) Post-indentation relative strength of the specimens versus the relative diameter of damage cone (comparison with results from Herb *et al.*[7]).

Figure 4a shows that equation (3) fits the strength data which indicates that the material is insensitive to impact damage. It means that there is no stress concentration induced by the presence of the impact cone. The σ_R strength dependence on a results instead from reduction in specimen section.

Figures 5a and 5b show the evolution of the linear density of acoustic events during monotonous loading. It can be noticed that acoustic emission was very significant in the zone of impact (*i.e.* between the dotted lines) for both samples at the beginning of loading (*i.e.* for strain level values between 0 and 0.10%). Failure did not occur under these strains but much later under larger deformation. Instead, under these larger strains, the AE activity in the impact area slowed down whereas it increased progressively in other parts of specimen, but looked quite homogeneous as load increased, indicating diffuse stress-induced damage. These results are consistent with impact damage insensitivity previously indicated. They indicate that the impacted specimens experience damage exactly like the as-received specimens under tensile load: stress driven diffuse matrix cracking and, in a second step, fibre failures.

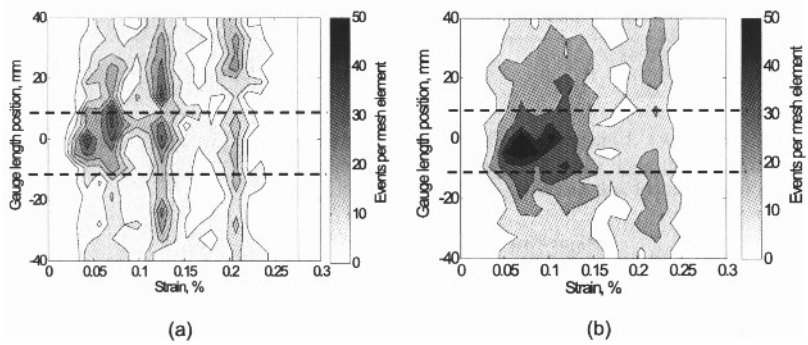

Figure 5. Evolution of linear densities of acoustic events along specimen axis during tensile tests at room temperature for the two impacted specimens (a) Impacted sample1. (b) Impacted sample2. The dotted lines bound the damage cone area.

Effect of impact-damage on static-fatigue

Very little deformation and damage were observed during fatigue on the as fabricated specimens. Besides, these specimens did not fail even after 1000 hours. Thus, the fatigue tests were interrupted and the tensile residual strength was measured at room temperature. The results are discussed below. As the static fatigue behaviour of SiC/SiC composites has been well documented in the literature[10,11] this part of the paper will focus on the impact-damaged specimens. Figures 6a and 6b compare the evolution of damage parameter ($D = 1 - E/E_0$) deduced from the strain measurements and the cumulative count of acoustic events. They highlight two interesting features.

First, the cumulative count of AE events mimics the evolution of damage under constant load. Second, damage and acoustic emission were less intense and quite constant at 650°C. This result demonstrates the effect of the self-healing matrix which protects the composite against oxidation at 650°C. Figure 7 shows also the location of AE events reflecting the occurrence of diffuse damage at 450°C as well as at 650°C. It is obvious on Figure 7 that acoustic emission was less intense at 650°C. The location of events is homogeneous all along the test, which agrees with the above-mentioned feature of stress-induced damage which is essentially diffuse, and also with the feature of notch insensitivity, since it does not appear a concentration of events in the vicinity of impact cone. Fig. 7 also shows significant slowing down of acoustic emission after 400 hours of static fatigue. This AE behaviour was observed at 450°C and 650°C. On Figures 7a and 7b, concentration of acoustic sources

was not detected during the first 400 hours. To check this result, the linear density of AE events was plotted on Figures 8 and 9.

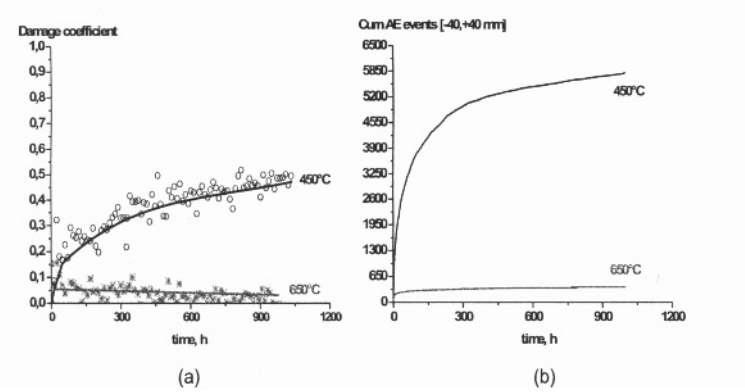

Figure 6. Plots of (a) evolution of damage parameter $D = 1 - E/E_0$ (b) cumulative count of acoustic events during static fatigue tests at 450°C and 650°C and under a constant stress (80 MPa) on impact-damaged specimens.

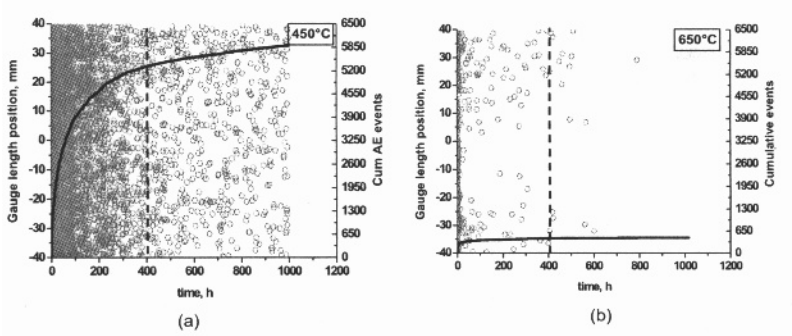

Figure 7. Location of the AE signals and the cumulative count of AE events in impact-damaged specimens during static fatigue tests under 80MPa, and at 450°C (a) and 650°C (b).

Figures 8 and 9 confirm that there was no acoustic activity concentration and that AE activity was less intense at 650°C. Nevertheless, in both cases, the impacted zone was more active at the beginning of tests, and then it was less active than the other parts of specimens after 100h. These results suggest that fatigue behaviour was not influenced by impact damage.

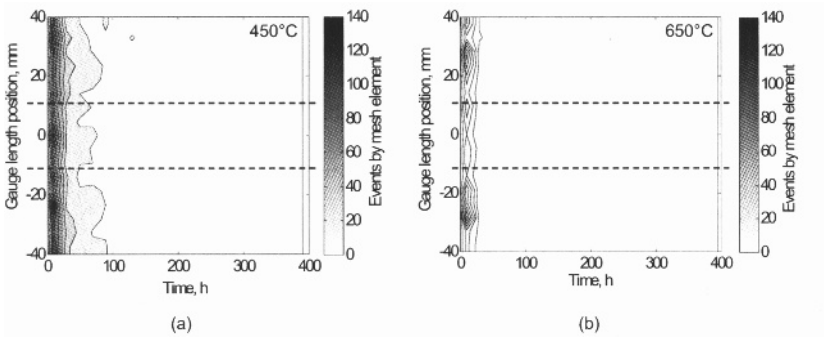

Figure 8. Linear density along specimen axis of AE events between 0 and 400 hours during static fatigue (a) at 450°C and (b) at 650°C. The dotted lines delineate the impact-damaged zone.

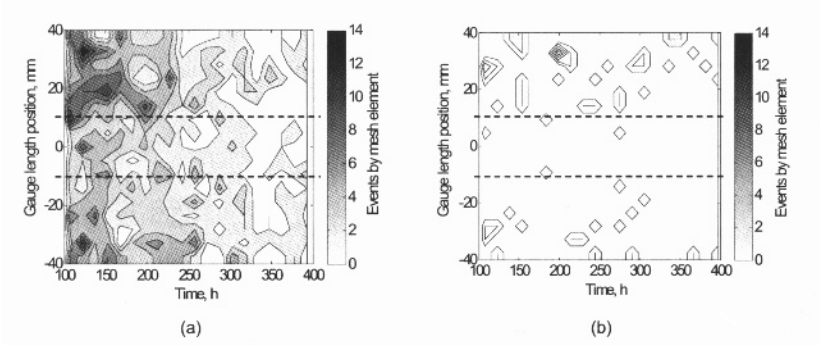

Figure 9. Linear density along specimen axis of AE events between 100 and 400 hours of static fatigue (a) at 450°C and (b) at 650°C. The dotted lines delineate the impact-damaged zone.

The impacted specimens did not break during the 1000 hours of static-fatigue whatever the test temperature. Residual strength was also measured using tensile tests at room temperature. Figure 10 compares initial and residual strengths for both as-fabricated specimens and impact-damaged specimens.

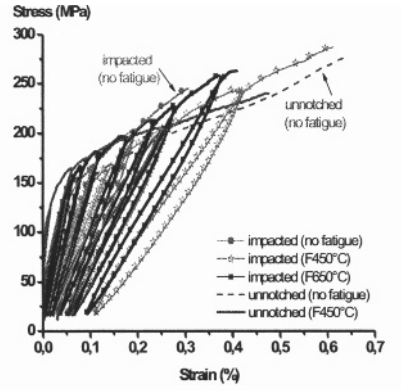

Figure 10. Comparison of the initial and residual tensile behaviour at room temperature of as-fabricated and impact-damaged specimens.

Though the tensile behaviour exhibits some variation (probably a material feature), the stress-strain curves highlight three important features. First, for both the as-fabricated and the impact-damaged specimens, the residual strengths were not significantly affected by fatigue tests at high temperature. Second, though material protection by matrix healing was not effective at 450°C, residual strength of the impacted specimens after 1000 hours of static fatigue was unchanged whatever the test temperature. Third, the residual failure stresses and strains for the impact-damaged specimens were close to those obtained on the as-fabricated samples after fatigue (Table 2). These features again indicate that under current experimental conditions the SiC/SiC composite fatigue behaviour was impact damage insensitive.

Table 2. Residual strengths and strains measured on specimens with or without impact damage after 1000 hours at 650°C and 450°C, under 80 MPa.

Sample	Failure strain (%)	Failure stress * (MPa)
Not-impacted (F450°C)	0.48	240
Impacted (F450°C)	0.61	288
Impacted (F650°C)	0.40	263

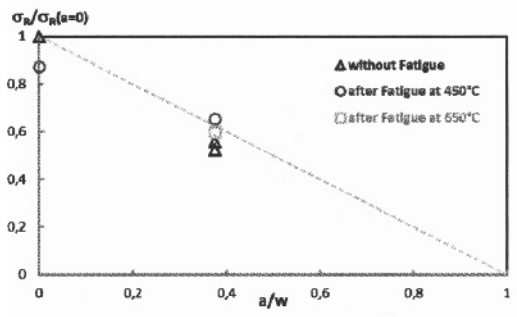

Figure 11. Relative residual strength of specimens versus the relative diameter of damage cone. Also given are the reference data of figure 4(b)

In order to assess the damage insensitivity of residual strengths, the data from tensile tests on specimens after fatigue were plotted on damage sensitivity diagram (figure 11). Figure 11 shows that the data pertain to the damage insensitivity line corresponding to equation (3) which agrees perfectly with the above results.

CONCLUSION

This paper investigated the effect of impact damage on SiC/SiC composite tensile behaviour at room temperature and static fatigue resistance at two intermediate temperatures (450°C and 650°C). Homemade software for post-treatment of AE signals from specimens gauge length during tests provided maps of linear density of acoustic events. These maps imaged damage during the tests. They showed that emission was intense near the impact cone at beginning of tests only. Specimens failed under larger strains. Their subsequent response was comparable to the non-linear mechanical behaviour of as-fabricated specimens. This observation illustrates the insensitivity to damage of this material, which is consistent with the notch insensitivity of long fibers reinforced composites[4].

Whatever the test temperature, no acoustic emission concentration was detected in the vicinity of impact cones during static fatigue at 80MPa. Under this stress the impacted specimens did not fail after 1000 hours. The ultimate strength of composite was not affected significantly by the fatigue tests whatever the sample was impact-damaged or not.

This work also confirms the effectiveness of the matrix self-healing process to protect the material against oxidation at 650°C. Investigation of lifetime of impact-damaged specimens at this temperature is in progress.

ACKNOWLEDGMENTS

The authors gratefully acknowledge DGCIS, Conseil Régional d'Aquitaine, DGAC, DGA, CNRS and Aerospace Valley for supporting this work in the frame of the program ARCOCE: "Arrière-Corps Composite Céramique, Ceramic Matrix Composites for Exhausts", and particularly P. Diss (SAFRAN, SNECMA Propulsion Solide) for fruitful discussions.

REFERENCES

[1] R. T. Bhatt, S. R. Choi, L.M. Cosgriff, D. S. Fox, K. N. Lee, Impact resistance of environmental barrier coated SiC/SiC composites, *Mater Sci Eng A*, **476**, 8–19 (2008).

[2] R. T. Bhatt, S. R. Choi, L.M. Cosgriff, D. S. Fox, K. N. Lee, Impact resistance of uncoated SiC/SiC composites. *Mater Sci Eng A*, **476**, 20-28 (2008).

[3] S. R. Choi, Foreign object damage phenomenon by steel ball projectiles in a SiC/SiC ceramic matrix composites at ambient and elevated temperatures. *J. Am. Ceram. Soc.*, **91**, 2963–8 (2008).

[4] S. R. Choi, D. J. Alexander R. W. Kowalik, Foreign object damage in an oxide/oxide composite at ambient temperature. *J. Eng. Gas. Turb. Power*, 131, 021301-1–0212301-6 (2009).

[5] M. Virelli, Impact Behavior of a SiC/SiC Composite at an Elevated Temperature, High Temperature Ceramic Materials and Composites (HTCMC-7), editors W. Krenkel and J. Lamon, AVISO Verlagsgesellschaft mbHD-10117 Berlin, Germany, 519–530 (2010).

[6] K. Ogi, T. Okabe, M. Takahashi, S. Yashiro, A. Yoshimura, T. Ogasawara, Experimental characterization of high-speed impact damage behaviour in a three-dimensionally woven SiC/SiC composite, *Composites: Part A*, **41**, 489–498 (2010).

[7] V. Herb, Damage assessment of thin SiC/SiC composite plates subjected to quasi-static indentation loading, *Composites: Part A* (2010) doi:10.1016/j.compositesa. 2010.08.004

[8] I. Berdoyes, J. Thebault, E. Bouillon, Improved SiC/SiC and C/C materials applications parts. In: Proceedings of the European congress on advanced materials and processes, EUROMAT 2005, Prague, Czech Republic, 5–8 September 2005.

[9] P. Tan, L. Tong, G. P. Steven, Modelling for predicting the mechanical properties of textile composites—a review. *Composite Part A*, **28A**, 903–22 (1997).

[10] S. Momon, M. Moevus, N. Godin, M. R'Mili, P. Reynaud, G. Fantozzi, G. Fayolle, Acoustic emission and lifetime prediction during static fatigue tests on ceramic-matrix-composite at high temperature under air, *Composites: Part A*, **41**, 913-918 (2010).

[11] M. Moevus, D. Rouby, N. Godin, M. R'Mili, P. Reynaud, G. Fantozzi, G. Fayolle, Analysis of damage mechanisms and associated acoustic emission in two SiC_f/[Si–B–C] composites exhibiting different tensile behaviours. Part II: Unsupervised acoustic emission data clustering, *Comp. Sc. and Tech.*, **68**, 1250-1257 (2008).

[12] G. N. Morscher, 1998. Modal acoustic emission of damage accumulation in a woven SiC/SiC composite, *Comp. Sci. Tech.*, **59**, 687-697 (1999).

[13] E. Maillet, N. Godin, M. R'Mili, P. Reynaud, J. Lamon, G. Fantozzi, Indicators of the critical behavior of Ceramic Matrix Composites for rupture time prediction during fatigue tests at intermediate temperatures, *Composite Science and Technology*, submitted.

[14] C. Droillard, J. Lamon, Fracture toughness of 2D woven SiC/SiC CVI-composites with multi-layered interphases, *J. Am. Ceram. Soc.*, **79**, 849-858 (1996).